

SHAPE OPTIMIZATION OF SHAFTS UNDER TORSION USING GENETIC ALGORITHMS AND BOUNDARY ELEMENTS

Daniela R. M. Araújo*

Afonso C. C. Lemonge

Luis P. S. Barra

{*daniela,lemonge,luisp*}@numec.ufff.br

* Bolsista de Iniciação Científica PIBIC CNPq/UFJF

NUMEC – Núcleo de Pesquisa em Métodos Computacionais em Engenharia

Universidade Federal de Juiz de Fora, Faculdade de Engenharia, Departamento de Estruturas

Campus Universitário, Bairro Martelos, CEP 36036-330, Juiz de Fora, MG, Brasil

Helio J.C. Barbosa

hcbm@lncc.br

Laboratório Nacional de Computação Científica – LNCC/MCT

Av. Getúlio Vargas, 333, Petrópolis, RJ, Brasil, CEP 25651-075

Abstract. *This paper discusses shape optimization problems for elastic shafts under torsion using genetic algorithms (GA) coupled to the boundary element method (BEM). A GA is proposed to evolve the shape optimization involving the objective function that minimizes the area of the cross-section where the constraint imposed is a minimum value of torsional stiffness. The design variables of the problem are coordinates of the nodes used to define the boundary element discretization of the cross section. These values are generated by the GA and handled by a mesh generator which defines a candidate solution to the problem. The value of the torsional stiffness for each individual is evaluated using an implementation of the direct boundary element method. For a given pair of values of cross-sectional area and torsional stiffness, the value of the fitness function of an individual is obtained. In this case the constrained optimization problem is replaced by an unconstrained one by means of a penalty function.*

In order to investigate the robustness of the proposed scheme, an optimization problem were tackled. The binary-coded generational GA uses a Gray code, rank-based selection, and elitism. Standard one-point, two-point, and uniform crossover as well a mutation operator were applied.

Keywords: *genetic algorithms, optimization, structural mechanics, boundary element method*

1. INTRODUCTION

Among the several possibilities of structural optimization, one that has deserved great attention is shape optimization, Mackerle (2003). In this type of problems, the aim is to determine the boundary geometry (or part of it) so that a certain quantity (objective function) is minimized (or maximized). For this purpose, it is necessary to solve the structural problem in question, determining the answers, in terms of displacement, deformations and stresses, for a specific requirement (or a set of them). This step is carried out by numerical methods such as the Finite Element Method (FEM), Hughes (1987), or the Boundary Element Method (BEM), C.A. Brebbia (1984).

Since the pioneering work of, Schmit (1960), several methodologies have been proposed and improved in the field of structural optimization. Techniques of mathematical programming are frequently used as the functions involved are nonlinear. Among them, the most efficient of these use gradient functions (that in the particular case of shape optimization are called sensibilities to changes in shape, or simply sensibilities), which are calculated with the aid of the numerical method used in the solution of the structural problem (FEM or BEM). A more recent alternative in dealing with optimization problems, which dispenses with obtaining the gradients of the functions, is Genetic Algorithms (GA), Goldberg (1989). This methodology is characterized by not requiring that the objective function be continuous or differential, not requiring complex formulations or reformulations for the problems, not requiring preliminary studies to defining start points, feasible or not, in the search space of solutions, being of an intrinsically parallel nature and of great flexibility in defining the objective function which can be easily modified without the necessity of extensive code rewriting.

This paper discusses shape optimization problems for elastic shafts, Gracia and Doblare (1988), under torsion using genetic algorithms (GA) coupled to the boundary element method (BEM), Annicchiarico and Cerrolaza (2002). The shape optimization problem considers sections under Saint-Venant torsion which can be solved by the Boundary Element Method.

A GA is proposed to evolve the shape optimization of the cross-section in order to minimize its area subject to a minimum value of the torsional stiffness.

The design variables of the problem are coordinates of the nodes used to define the boundary element discretization of the cross section. These values are generated by the GA and handled by a mesh generator which defines a candidate solution to the problem. The value of the torsional stiffness for each individual is evaluated using an implementation of the direct boundary element method.

For a given pair of values of cross-sectional area and torsional stiffness, the value of the fitness function of an individual is obtained. In this case the constrained optimization problem is replaced by an unconstrained one by means of a penalty function.

In order to investigate the robustness of the proposed scheme, an optimization problem were tackled. The binary-coded generational GA uses a Gray code, rank-based selection, and elitism. Standard one-point, two-point, and uniform crossover as well a mutation operator were applied.

2. Torsion of Prismatic Bars by BEM

The equations describing a linear elastic prismatic bar in torsion as depicted in Figure 1 and 2 can be stated by means of the so called Saint-Venant stress function, $\phi(x_1, x_2)$, such that Timoshenko and Goodier (1970):

$$\begin{aligned}\tau_{13} &= \alpha G \phi_{,2} \\ \tau_{23} &= -\alpha G \phi_{,1}\end{aligned}\tag{1}$$

where the comma represents spatial derivatives and G is the shear modulus of the material.

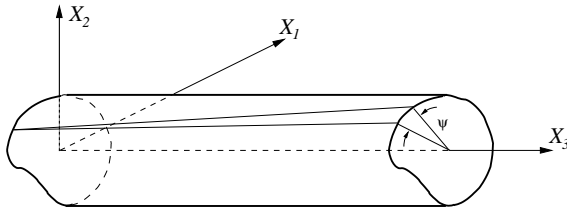


Figure 1: Prismatic bar under torsion.

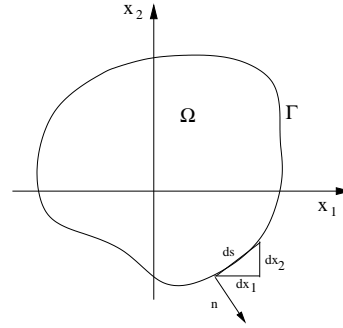


Figure 2: Normal vector to the boundary of transversal section of the bar.

In this way, the equilibrium equations are identically satisfied and the compatibility equations become:

$$\phi_{,11} + \phi_{,22} \equiv \phi_{,ii} = -2 \quad (2)$$

The boundary conditions of the problem imply that

$$\tau_{13}n_1 + \tau_{23}n_2 = 0 \quad (3)$$

where n_i are the components of the unit normal vector \mathbf{n} which means that the resultant shearing stress at the boundary is tangent to the boundary.

Using the relations:

$$n_1 = \cos(n, x_1) = \frac{dx_2}{ds}$$

$$n_2 = \cos(n, x_2) = -\frac{dx_1}{ds} \quad (4)$$

the following equation are then obtained:

$$\alpha G \phi_{,1} \cdot \frac{dx_1}{ds} + \alpha G \phi_{,2} \cdot \frac{dx_2}{ds} \equiv \alpha G \frac{d\phi}{ds} = 0 \quad (5)$$

In other words, the stresses function $\phi(x_1, x_2)$ must be constant along the whole section boundary, Γ . In simply connected domains this constant is immaterial and has been set to zero here, i.e.:

$$\phi = 0 \quad \text{in } \Gamma. \quad (6)$$

The resultant of the forces distributed over the ends of the bar is zero, and these forces represent a torque couple of magnitude:

$$M = \int_{\Omega} (\tau_{23} x_1 - \tau_{13} x_2) dx_1 dx_2 = -\alpha G \int_{\Omega} (\phi_{,1} x_1 + \phi_{,2} x_2) dx_1 dx_2 \quad (7)$$

Observing the above equation, the torque needed to promote a unit rotation per unit length, α , the torsion stiffness, D is:

$$D = -G \int_{\Omega} (\phi_{,1} x_1 + \phi_{,2} x_2) dx_1 dx_2 \quad (8)$$

Once the problem is stated as the Poisson equation in Ω , subjected to the boundary condition (6), it can be easily solved by several numerical methods.

In the present work a standard direct formulation of the BEM, Brebbia et al. (1984), was used due to its good results and simplicity in treating the necessary remeshing. The method is based on the discretization of following integral equation for a generic body force term $b(x)$:

$$c(\xi) \phi(\xi) + \oint_{\Gamma} \frac{d\phi^*}{dn}(\xi, x) \phi(x) d\Gamma - \int_{\Gamma} \phi^*(\xi, x) \frac{d\phi^*}{dn}(x) d\Gamma + \int_{\Omega} \phi^*(\xi, x) b(x) d\Omega \quad (9)$$

where $\xi \in \Gamma$, and the integral \oint_{Γ} should be understood in the sense of principal value. The functions $\phi^*(\xi, x)$ and $\frac{d\phi^*}{dn}(\xi, x)$ correspond to the exact solution of the problem in an unbounded domain, forced by a unit point source at ξ :

$$\phi^*(\xi, x) = -\frac{1}{2\pi} \ln(r) \quad (10)$$

$$\frac{d\phi^*}{dn}(\xi, x) = -\frac{1}{2\pi} r_{,i} n_i \quad (11)$$

As in the present problem $b(x) = -2$, the domain integral in the above expression can be rewritten as a boundary integral:

$$\int_{\Omega} \phi^*(\xi, x) b d\Omega = b \int_{\Gamma} v_{,i}^* n_i(\xi, x) d\Gamma \quad (12)$$

where

$$v_{,i}^*(\xi, x) = -\frac{1}{2} \left(\frac{1}{4\pi} + u^*(\xi, x) \right) r_{,i}$$

In order to avoid domain discretization, the torsion stiffness and cross sectional area were also written as boundary integrals by means of the divergence theorem, Barra (1990), as:

$$A = \int_{\Gamma} x_i n_i d\Gamma \quad (13)$$

$$D = -\frac{G}{2} \int_{\Gamma} R^2 \left(\phi_{,i} + \frac{x_i}{2} \right) n_i d\Gamma \quad (14)$$

2.1 GENETIC ALGORITHMS

One reason for GA's popularity is that, unlike many traditional optimization methods, when used as a minimization (or maximization) algorithm it differs from the more familiar mathematical programming techniques by (i) employing a *population* of candidate solutions, (ii) operating upon the *coding* of a solution and not on the solution itself, (iii) using *probabilistic* transition rules, and (iv) not requiring additional information (like derivatives) about the function to be optimized. As a result, the search can be performed over non-convex (and even disjunct) sets for non-convex, non-differentiable functions of variables that can be continuous and/or discrete. The first step is to encode all the variables corresponding to a candidate solution in a chromosome. In this paper we adopted the standard binary coding: each variable is encoded into a string of binary digits of a convenient length and these strings are then concatenated to form a single string which is an individual in the population of candidate solutions. A linear *rank-based* selection scheme is adopted. Given the current population, this selection scheme starts

by sorting the population according to the values of the fitness function constructing a *ranking*, i.e. better solutions have higher rank. Individuals in the population are then selected in such a way that higher ranking individuals have a higher probability of being chosen for reproduction. This leads to an intermediate population whose elements will then be operated upon by the recombination and mutation operators. The recombination of the genetic material of the selected “parent” chromosomes in order to generate the offspring chromosomes will be accomplished here using three *crossover* operators – one-point, two-point and uniform, Syswerda (1995). The recombination operation is usually performed with a user-defined probability p_c and, consequently, with probability $1 - p_c$, the operation is not performed and both parents are just copied and sent to the mutation operation step. After the recombination step and again inspired in Nature, a mutation operator is introduced to simulate the errors that may arise during the copy process. With a (low) given mutation rate p_m the mutation operator is applied to each bit in the offspring chromosomes. The effect of this operator in the case of a binary alphabet is simple: just change a 1 into a 0 and vice-versa. After a new population is created each individual/solution must be evaluated in order to have a fitness value assigned to it. The BEM is then used to generate the mesh and compute the values of the area and the torsional stiffness of each candidate solution.

3. NUMERICAL EXPERIMENTS

In order to investigate the robustness of the proposed optimization procedure, a numerical experiment is discussed. A GA is proposed to evolve the shape optimization involving the objective function that minimizes the area of the cross-section where the constraint imposed is a minimum value of the torsional stiffness.

The GA proposed can be stated as:

```

begin
Initialize the population P
Generate the boundary element for each string
Evaluate each string in the population
repeat
  repeat
    Select 2 or more individuals in P
    Apply recombination operators with probability  $p_c$ 
    Apply mutation operator with rate  $p_m$ 
    Insert new individuals in P'
  until (population P' complete)
  Evaluate individuals in population P'
  P ← P'
until (termination criterion)
stop
end

```

The optimization tool implemented uses a GA and a Boundary Element Method (BEM) codes and both work independently.

The design variables of the problem are the coordinates of the nodes used to define the boundary element discretization of the shaft as shown in the Figure 3. The exact solution of the problem analyzed in this experiment is given by a circular section with radius $R = 10$ (area equal to 314.159), and torsional stiffness $D = 15707.96327$.

Two cases are analyzed in this problem: the first one corresponds to a parametrization of the cross-section without any type of symmetry considered, and the second case considers

the double symmetry presented in this problem. The first case is discretized with 24 design variables ($x_i, i = 1,24$), whereas the second one is discretized with 7 design variables ($x_1, x_2, x_3, x_4, x_{13}, x_{14}$ and x_{15}) as can be observed in the Figure 3.

For both cases, 12 contours were defined and each one of them containing three points: the initial point, the final point and the middle point. The first contour is defined by the points 1, 2 and 3 and the twelfth by the points 12, 1 and 24. It is important to note that the angle between each direction assigned to a design variable is equal to $\pi/12$. To obtain the complete mesh for the BEM 8 elements were generated between the initial and final points of each contour and, consequently, the mesh is made up of 96 boundary elements. From this point x is considered a

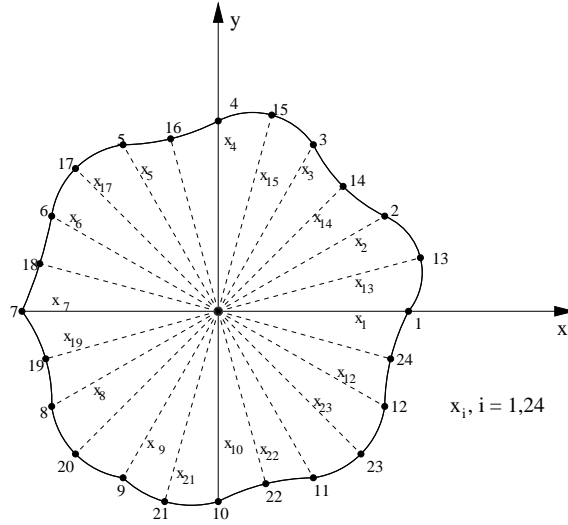


Figure 3: Design variables.

design variable in the following expressions. The objective function (to be minimized), can be written as:

$$f(x) = A = \int_{\Gamma} x_i n_i d\Gamma \quad (15)$$

The fitness function can be stated as:

$$F(x) = f(x) + \alpha \left(\left[1 - \frac{D(x)}{\bar{D}} \right]^+ \right)^2 \quad (16)$$

where $D(x)$ is the torsional stiffness of the current candidate solution x , \bar{D} is the constraint (given torsional stiffness), and α is a constant penalty coefficient which was set to 10^4 in all experiments.

3.1 The first case - without symmetry.

For the first case, the parameters of the GA are:

- Number of runs: 10;
- Number of design variables: 10;
- Population size: 60;
- Chromosome length: 240 bits (10 bits per design variable);

- Maximum number of generations: 100;
- Crossover probability: $p_r = 0.8$;
- Mutation probability: $p_r = 0.03$;
- Lower bound of the design variables: 9;
- Upper bound of the design variables: 11.

The Table 1 shows the best feasible solutions found in 10 independent runs where $F(x)$ is the value of fitness function (equal to the objective function = area of the shaft). All of these values are very close to the exact solution with respect to both the area (314.159) and the torsional stiffness $D(x) = 15707.96327$. It is important to note that the values of D are greater than 15707.96327. Among them the best solution was found in the second run with values $F(x) = 314.64$ and $D(x) = 15709.5$. Differently of the Table 1, the Table 2 shows the best infeasible solutions found in the same 10 independent runs. Although infeasible, all of these values are very close to the exact solution with respect to both the area (314.159) and the torsional stiffness $D(x) = 15707.96327$. Among them the best solution was found in the ninth run with values $F(x) = 313.93$ and $D(x) = 15609.8$. This is the greatest value of D among these solutions and, naturally, the smaller violation of the imposed constraint.

Table 1: Design variables for the best feasible solutions and the corresponding values of the objective function $f(x)$ and the torsional stiffness $D(x)$ in 10 independent runs.

Var	Run 1	Run 2	Run 3	Run 4	Run 5	Run 6	Run 7	Run 8	Run 9	Run 10
1	9.97	9.72	9.32	9.94	10.17	10.52	10.10	9.52	10.26	9.78
2	9.98	9.45	9.71	9.83	10.07	10.28	10.47	9.85	10.00	10.09
3	9.86	9.44	10.01	9.97	9.98	10.02	10.34	10.31	9.80	10.21
4	9.95	9.71	10.29	9.94	9.98	10.01	10.01	10.19	9.69	10.43
5	9.51	9.67	10.26	9.78	9.83	9.88	10.29	9.99	9.50	10.54
6	9.63	9.91	10.46	10.18	9.90	9.66	10.18	10.39	9.65	10.28
7	9.79	9.82	10.47	10.40	9.93	9.33	10.01	9.93	9.85	10.22
8	9.42	9.80	10.30	10.63	9.99	9.39	10.05	10.02	9.87	10.13
9	9.76	9.82	10.18	10.35	9.48	9.33	10.21	10.19	10.07	9.83
10	10.08	10.17	10.10	10.34	9.84	9.51	10.00	10.54	10.09	9.41
11	10.30	10.00	10.02	10.33	9.81	9.69	10.42	10.35	9.48	9.37
12	10.24	10.46	10.28	10.52	9.98	9.79	10.15	10.35	9.62	9.50
13	10.46	10.24	10.06	10.08	10.06	10.18	10.06	10.41	9.90	9.83
14	10.02	10.44	10.13	9.89	10.21	10.23	9.92	10.14	9.69	9.88
15	10.10	10.39	10.19	9.50	10.02	10.10	9.76	9.93	9.99	9.39
16	9.96	10.38	10.22	9.43	9.90	10.15	9.74	9.97	9.89	9.70
17	9.88	10.10	10.26	9.50	9.71	10.08	9.68	9.85	10.13	9.81
18	9.93	10.20	10.18	9.65	10.06	10.26	9.37	9.82	10.21	10.20
19	10.03	9.77	9.90	10.07	10.20	10.35	9.72	9.67	10.39	10.44
20	10.07	10.08	9.93	9.94	10.22	10.43	9.86	9.93	10.65	10.46
21	10.57	10.12	9.52	9.93	10.12	10.38	10.47	9.61	10.18	10.29
22	10.50	10.09	9.45	9.90	10.16	10.03	9.91	9.71	10.34	10.02
23	10.27	10.15	9.11	9.93	10.19	10.38	9.96	9.72	10.39	10.13
24	10.21	9.84	9.47	10.06	10.14	10.26	10.06	9.52	10.53	10.26
$F(x)$	314.98	314.64	314.77	314.88	314.71	314.71	314.99	314.78	314.94	315.14
D	15720.2	15709.5	15713.8	15716.0	15727.6	15718.5	15718.7	15710.5	15718.1	15716.0

The Figure 4 shows the final shape of the shaft for the best feasible solution found in the first run. The Figure 5 shows the final shape of the best infeasible solution found in the sixth run. The red color in both cases corresponds to the exact solution whereas the blue color indicates the solutions found by the GA. One can conclude that these solutions are very reasonable.

The Figures from 6 to 8 present, for each individual in the population, the value of the objective function and the respective value of the fitness function in the initial population and generations 30 and 60. The minimum value of the torsional stiffness is also plotted in these

Table 2: Design variables for the best infeasible solutions and the corresponding values of the objective function $f(x)$ and the torsional stiffness $D(x)$ in 10 independent runs.

Var	Run 1	Run 2	Run 3	Run 4	Run 5	Run 6	Run 7	Run 8	Run 9	Run 10
1	10.03	9.72	9.31	9.94	10.06	10.39	10.09	9.70	10.26	9.97
2	9.94	9.42	9.71	9.91	10.05	10.29	10.44	9.85	10.00	10.09
3	9.89	9.44	10.01	9.97	9.98	10.01	10.31	9.69	9.98	10.22
4	9.80	9.71	10.23	9.93	9.98	10.01	10.11	10.22	9.68	10.43
5	9.51	9.67	10.26	9.78	9.92	9.62	10.22	9.94	9.51	10.53
6	9.34	9.84	10.46	10.15	9.83	9.35	9.82	10.32	9.65	10.28
7	9.71	9.82	10.47	10.40	9.92	9.42	9.99	9.82	9.79	10.21
8	9.42	9.80	10.33	10.63	10.01	9.39	10.06	10.02	9.85	10.13
9	9.76	9.82	10.08	10.33	9.49	9.33	10.18	10.19	9.93	9.79
10	9.92	10.17	9.98	10.32	9.83	9.51	10.01	10.53	9.82	9.42
11	10.20	10.00	10.02	10.33	9.83	9.63	10.17	10.35	9.48	9.37
12	10.24	10.46	10.28	10.51	9.88	9.83	10.16	10.28	9.60	9.53
13	10.45	10.24	10.07	10.05	10.06	10.09	10.05	10.34	9.65	9.66
14	10.23	10.44	10.13	9.89	10.20	10.17	9.92	10.11	9.69	9.88
15	10.10	10.39	10.19	9.75	10.04	10.09	9.76	9.93	9.88	9.64
16	9.96	10.43	10.22	9.46	9.90	10.15	9.72	9.97	9.89	9.71
17	9.87	10.12	10.26	9.52	9.79	10.08	9.82	9.84	10.13	9.82
18	9.93	10.20	10.18	9.63	10.05	10.26	9.37	9.80	10.27	10.20
19	10.03	9.77	9.90	10.07	10.14	10.34	9.72	9.83	10.38	10.32
20	10.07	10.08	9.92	9.94	10.16	10.43	9.76	9.87	10.68	10.31
21	10.59	10.11	9.52	9.58	10.13	10.38	10.46	9.61	10.32	10.32
22	10.50	9.92	9.30	9.60	10.15	10.11	10.07	9.71	10.42	10.14
23	10.23	9.90	9.11	9.93	10.29	10.38	9.97	9.75	10.35	10.13
24	10.24	9.82	9.47	10.05	9.91	10.26	10.06	9.65	10.40	9.74
$F(x)$	314.17	313.95	314.16	314.25	313.92	313.91	314.21	314.03	313.93	314.22
D	15578.0	15591.0	15593.0	15584.6	15577.2	15566.1	15600.6	15590.5	15609.8	15590.0

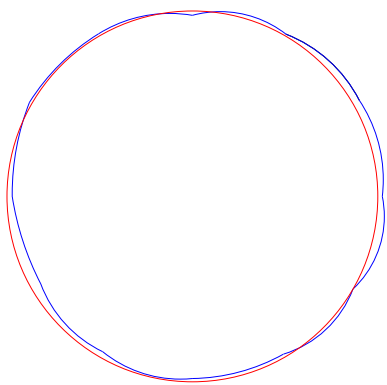


Figure 4: Best feasible solution found in the first run – Area = 314.64 and Torsional stiffness = 15709.5.

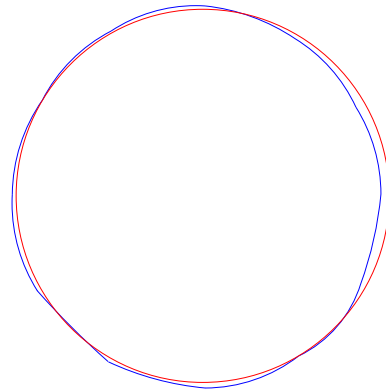


Figure 5: Best infeasible solution found in the sixth run – Area = 313.91 and Torsional stiffness = 15566.1.

graphs. Observing them one can note that along the evolution there is a trend in the population, to approach this constraint. Besides, in the end of the process there are feasible as well as infeasible solutions. The other set of Figures from 9 to 10 show the comparison between the objective and fitness functions. The feasible elements of the population have the same values for both functions and in those graphs they appear above the constraint. The elements below this line are infeasible. Since the penalty function increases the value of the objective function and grows with the value of the violation, it is interesting to observe that the “most infeasible” solution (smaller objective function) has the greatest value of the fitness function. Along the evolution there is a trend in the population to approach the limit between the feasible and infeasible design spaces.

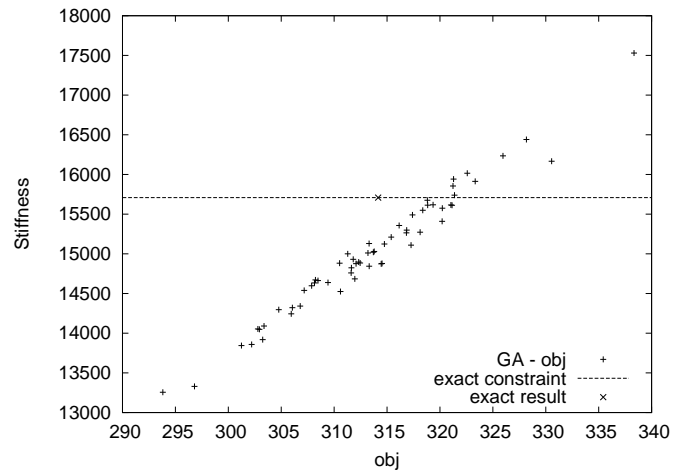


Figure 6: Objective function – Initial population.

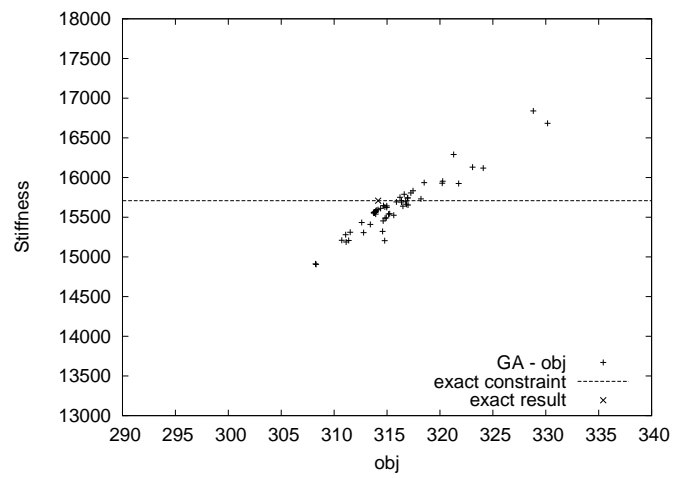


Figure 7: Objective function – Generation 30.

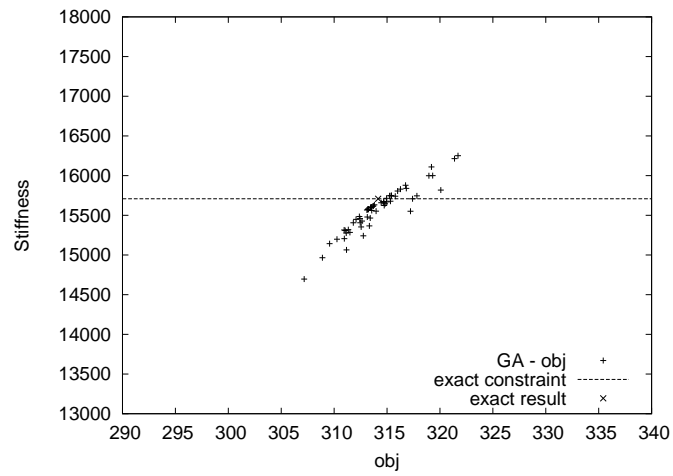


Figure 8: Objective function – Generation 60.

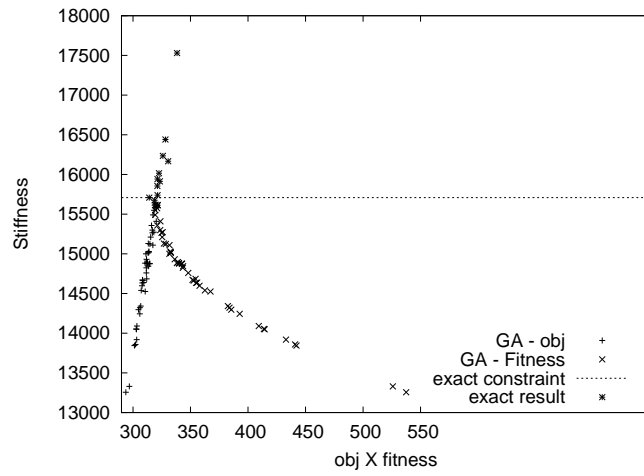


Figure 9: Objective and Fitness function – Initial population.

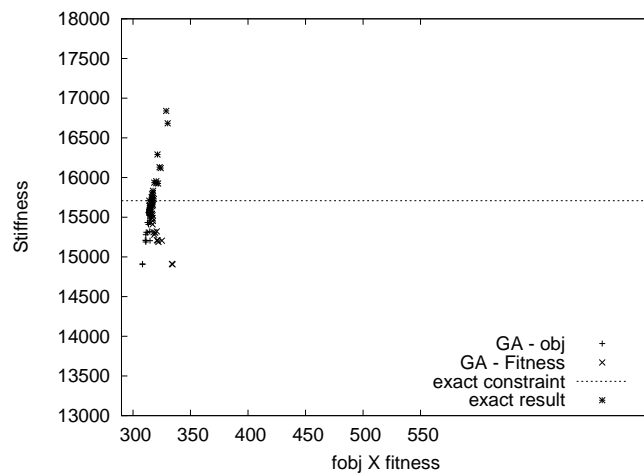


Figure 10: Objective and Fitness function – Generation 30.

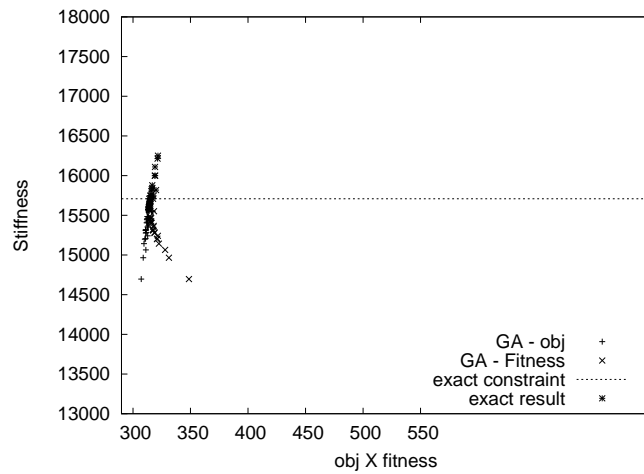


Figure 11: Objective and Fitness function – Generation 60.

3.2 The second case - with symmetry.

In order to experiment the characteristics of the symmetry present in this particular example the number of design variables was reduced from 24 to 7 and only one quarter of the geometry was considered. In this case, the parameters of the GA are:

- Number of runs: 10;
- Number of design variables: 7;
- Population size: 60;
- Chromosome length: 70 bits (10 bits per design variable);
- Maximum number of generations: 100;
- Crossover probability: $p_r = 0.8$;
- Mutation probability: $p_r = 0.03$;
- Lower bound of the design variables: 9;
- Upper bound of the design variables: 11.

As in the previous case, the Table 3 shows the best feasible solutions found in 10 independent runs where $F(x)$ is the value of fitness function (equal to the objective function = area of the shaft). All of these values are very close to the exact solution with respect to both the area (314.159) and the torsional stiffness $D = 15707.96327$. It is important to note that the values of D are greater than 15707.96327. Among them the best solution was found in the seventh run with $F(x) = 314.24$ and $D(x) = 15708.1$ and this one is better than the feasible solution, as expected, found in the previous case. In the same way the Table 4 shows the best infeasible solutions found in the same 10 runs. Although infeasible, all of these values are very close to the exact solution and among them the best solution was found in the ninth run with $F(x) = 313.79$ and $D(x) = 15592.4$. This is the greatest value of D among these solutions and, naturally, the smaller violation of the imposed constraint.

Table 3: Design variables for the best feasible solutions and the corresponding values of the objective function $f(x)$ and the torsional stiffness $D(x)$ in 10 independent runs.

Var	Run 1	Run 2	Run 3	Run 4	Run 5	Run 6	Run 7	Run 8	Run 9	Run 10
1	10.03	9.83	9.89	10.05	9.96	10.06	10.07	10.12	9.85	10.01
2	9.91	9.89	9.99	9.97	9.99	10.03	9.96	10.04	9.78	9.99
3	9.98	9.85	10.02	10.05	9.84	9.94	9.90	10.14	10.17	10.07
4	10.04	10.07	10.01	9.98	10.05	10.00	9.99	10.01	9.98	9.97
5	10.01	10.13	9.99	9.97	10.02	10.09	10.01	9.94	10.11	10.03
6	10.05	10.11	10.07	10.06	10.04	9.98	10.07	9.93	10.24	9.99
7	10.08	10.03	9.93	9.93	10.09	9.94	10.10	9.89	10.86	10.02
$F(x)$	314.24	314.33	314.24	314.28	314.3	314.25	314.24	314.27	318.8	314.25
D	15709.3	15708.9	15708.4	15711.4	15710.0	15708.8	15708.1	15710.5	16079.6	15712.2

The Figure 12 shows the final shape of the shaft for the best feasible solution found in the first run. The Figure 13 shows the final shape of the best infeasible solution found in the sixth run. The red color in both cases corresponds to the exact solution whereas the blue color indicates the solutions found by the GA. One can conclude that these solutions are very good. These shapes are very close to the exact shape of this problem and, as expected, the symmetry adopted leads to better solutions.

The Figures from 14 to 16 present, for each individual in the population, the value of the objective function and the corresponding value of the fitness function in the initial population and generations 30 and 60. The minimum value of the torsional stiffness is also plotted in these

Table 4: Design variables for the best infeasible solutions and the corresponding values of the objective function $f(x)$ and the torsional stiffness $D(x)$ in 10 independent runs.

Var	Run 1	Run 2	Run 3	Run 4	Run 5	Run 6	Run 7	Run 8	Run 9	Run 10
1	9.98	9.83	9.98	10.00	9.98	10.06	9.93	10.00	9.72	9.98
2	9.91	9.90	9.99	9.96	9.94	10.00	9.92	10.04	9.78	10.00
3	9.98	9.87	10.02	9.98	9.94	9.95	9.91	10.00	9.83	9.95
4	9.96	10.06	10.01	9.92	9.97	10.00	9.99	10.00	9.99	9.97
5	10.01	10.12	9.98	10.00	10.00	9.96	10.03	9.97	10.08	10.03
6	10.05	10.02	9.95	10.06	10.04	9.98	10.06	9.93	10.24	9.99
7	10.07	10.03	9.95	9.99	10.06	9.94	10.03	9.89	10.23	9.98
$F(x)$	313.59	313.68	313.57	313.61	313.58	313.58	313.59	313.58	313.79	313.58
D	15584.1	15581.5	15585.1	15579.5	15584.0	15582.9	15585.4	15588.1	15592.4	15594.4

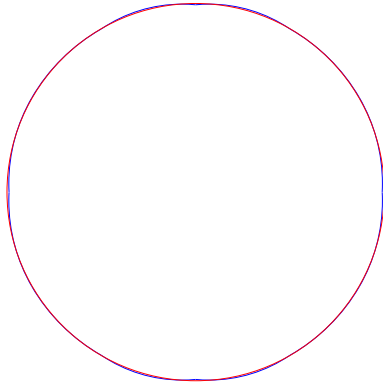


Figure 12: Best feasible solution found in the third run – Area = 314.24 and Torsional stiffness = 15708.4.

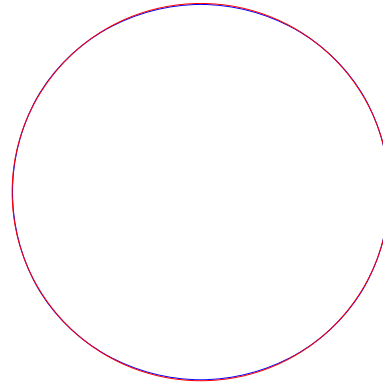


Figure 13: Best infeasible solution found in the third run – Area = 313.57 and Torsional stiffness = 15585.1.

graphs. Observing them one can note that along the evolution, as in the previous experiment without symmetry, there is a trend in the population to approach this constraint value. Again, in the end of the process there are feasible as well as infeasible solutions in the population. Finally, the other set of Figures from 17 to 19 show the comparison between the objective and fitness functions.

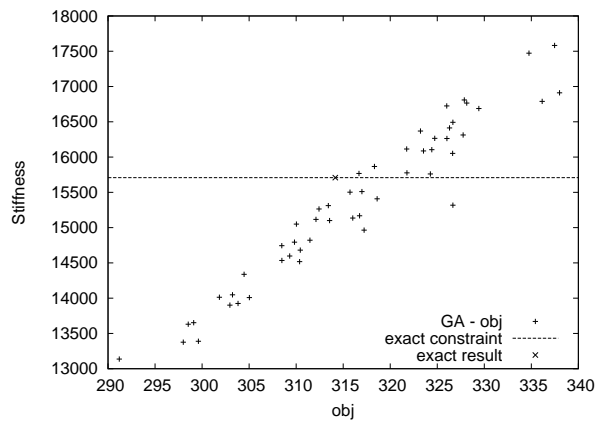


Figure 14: Objective function – Initial population.

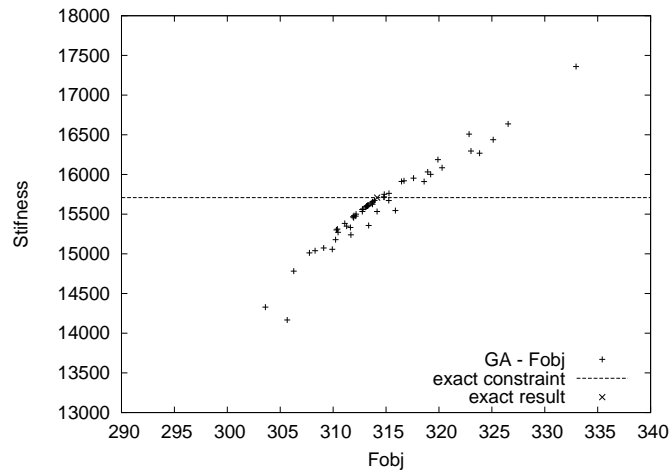


Figure 15: Objective function – Generation 30.

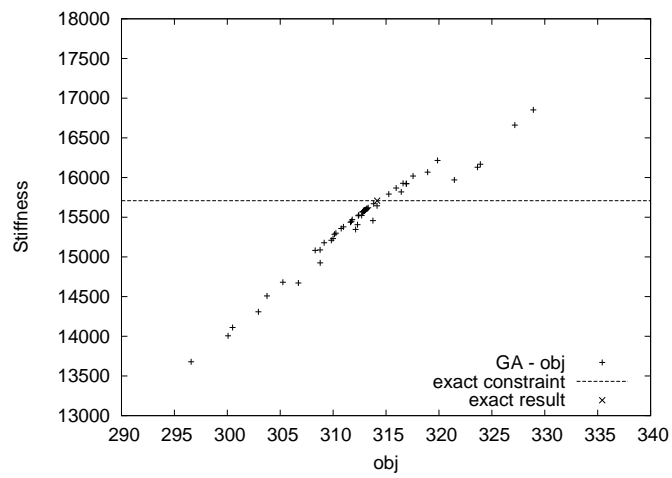


Figure 16: Objective function – Generation 60.

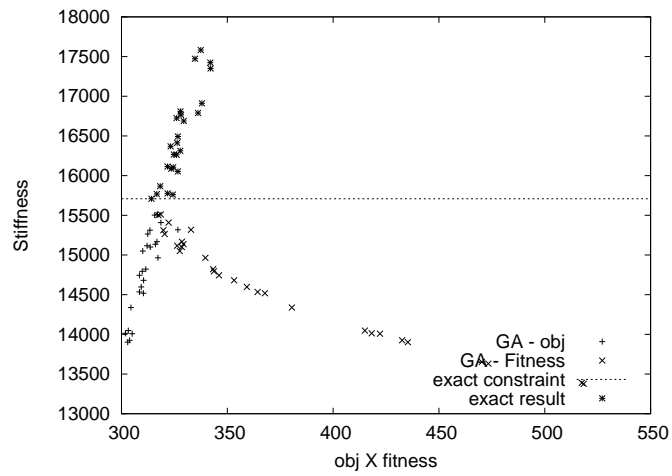


Figure 17: Objective and fitness function – Initial population.

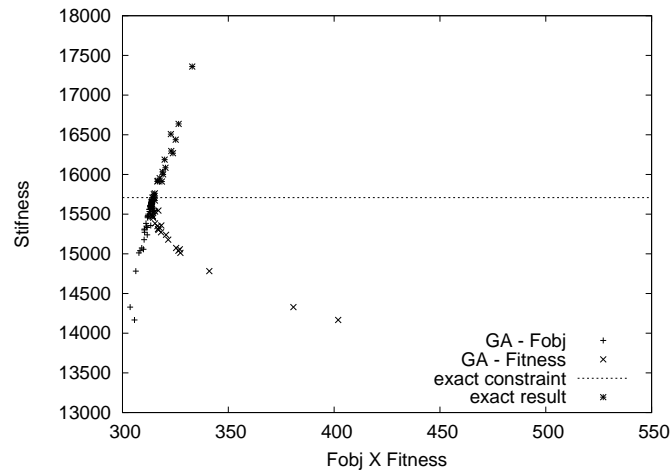


Figure 18: Objective and fitness function – Generation 30.

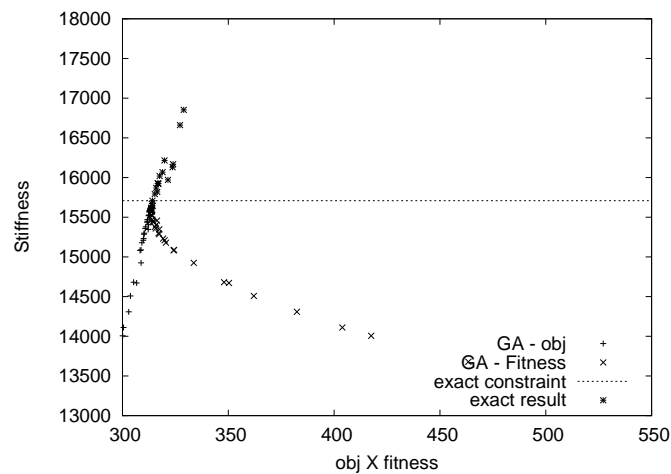


Figure 19: Objective and fitness function – Generation 60.

3.3 CONCLUSIONS

The results presented in this work correspond to the first experiments performed with the GA+BEM optimization tool implemented. They might be considered very simple but the structure of the codes worked very well and it provides a means to experiment with other types of problems where the BEM can be applied with success.

The example discussed in this text will be tested varying the set of parameters of the GA –number of runs, population size, probabilities, operators, etc– as well as the characteristics that defines the boundary element mesh as the number of contours, the type of element, number of integration points, etc.

Besides, spline curves, Blanc and Schlick (1995), have been implemented to better represent the contour of the domains and enabling the analysis of optimization problems presenting complex geometries.

Acknowledgments

The authors acknowledge the support received from PIBIC/UFJF-CNPq (Programa de Bolsas de Iniciação Científica, Universidade Federal de Juiz de Fora).

REFERENCES

- Annicchiarico, W. & Cerrolaza, M., 2002. An evolutionary approach for the shape optimization of general boundary elements models. *Electronic Journal of Boundary Elements*, vol. BETEQ2001, n. 2, pp. 251–266.
- Barra, L., 1990. *Cálculo de Sensibilidades – Uma Aplicação dos Elementos de Contorno à Otimização de Forma*. PhD thesis, Programa de Engenharia Civil da COPPE/UFRJ, Rio de Janeiro, Brasil.
- Blanc, C. & Schlick, C., 1995. X-splines: A spline model designed for the end-user. In *Proc. of SIGGRAPH'95*.
- Brebbia, C., Telles, J., & Wrobel, L., 1984. *Boundary Element Techniques – Theory and Applications in Engineering*. Springer-Verlag.
- C.A. Brebbia, J. T. e. L. W., 1984. *Boundary Element Techniques - Theory and Applications in Engineering*. Springer-Verlag.
- Goldberg, D., 1989. *Genetic Algorithms in Search, Optimization and Machine Learning*. Addison-Wesley Pub. Co.
- Gracia, L. & Doblare, M., 1988. Shape optimization of elastic orthotropic shafts under torsion by using boundary elements. *Computers & Structures*, vol. 30, n. 6, pp. 1281–1291.
- Hughes, T., 1987. *The Finite Element Method: Linear Static and Dynamic Finite Element Analysis*. Prentice Hall, Inc., Eaglewood Cliffs, New Jersey.
- Mackerle, J., 2003. Topology and shape optimization of structures using fem and bem a bibliography (1999-2001). *Finite Element Analysis and Design*, vol. 39, n. 3, pp. 243–253.
- Schmit, L., 1960. Structural design by systematic sythesis. In ASCE, ed, *Proceedings of the Second Conference on Eletronic Computation*, pp. 105–122, New York. ASCE.
- Syswerda, G., 1995. Uniform crossover in genetic algorithms. In Shaffer, J., ed, *Third International Conference on Genetic Algorithms and Their Applications*, pp. 2–9. Morgan Kaufmann, San Mateo, CA.
- Timoshenko, S. & Goodier, J., 1970. *Theory of Elasticity*. McGraw-Hill International editions.